

## Identification of Nucleolin as an AU-rich Element Binding Protein Involved in *bcl-2* mRNA Stabilization\*

Received for publication, August 18, 2003, and in revised form, December 4, 2003  
Published, JBC Papers in Press, December 16, 2003, DOI 10.1074/jbc.M309111200

Tapas K. Sengupta‡§, Sumita Bandyopadhyay‡§, Daniel J. Fernandes‡, and Eleanor K. Spicer‡||

From the ‡Department of Biochemistry and Molecular Biology and ¶Department of Pharmaceutical Sciences, Medical University of South Carolina, Charleston, South Carolina 29425

*bcl-2* mRNA contains an AU-rich element (ARE) that functions in regulating *bcl-2* stability. Our earlier studies indicated that taxol- or okadaic acid-induced *bcl-2* mRNA destabilization in HL-60 cells is associated with decreased binding of *trans*-acting factors to the ARE. To identify factors that play a role in the regulation of *bcl-2* mRNA stability, *bcl-2* ARE-binding proteins were purified from HL-60 cells. Three polypeptides of 100, 70, and 32 kDa were isolated from a *bcl-2* ARE affinity matrix. Matrix-assisted laser desorption ionization mass spectroscopy analysis identified these proteins as full-length nucleolin and proteolytic fragments of nucleolin. RNA gel shifts assays indicated that recombinant nucleolin (residues 284–707) binds specifically to *bcl-2* ARE RNA. In addition, recombinant nucleolin decreases the rate of decay of mRNA in HL-60 cell extracts in an ARE-dependent manner. Taxol or okadaic acid treatment of HL-60 cells results in proteolysis of nucleolin in a similar time frame as drug-induced *bcl-2* mRNA down-regulation. These findings suggest that nucleolin functions as a *bcl-2*-stabilizing factor and that taxol and okadaic acid treatment induces apoptosis in HL-60 cells through a process that involves down-regulation of nucleolin and destabilization of *bcl-2* mRNA.

The mammalian *bcl-2* gene encodes a 29-kDa protein that functions as an inhibitor of programmed cell death or apoptosis. Overexpression of *bcl-2* is thought to be an important component in the development of B cell lymphomas and certain leukemias (1, 2). In addition to its importance in cancer development, high *bcl-2* expression in hematological tumors is frequently an obstacle to cancer chemotherapy (3, 4). Numerous reports describe the effects of anti-cancer and apoptotic agents on the steady state levels of *bcl-2* mRNA and Bcl-2 protein (3, 5–7). For example, taxol induces apoptosis in ovarian cancer cells through a process that involves *bcl-2* mRNA destabilization (5). Similarly, okadaic acid (OA)<sup>1</sup>-induced apoptosis of human HL-60 leukemia cells is preceded by destabilization of

*bcl-2* mRNA as well as down-regulation of Bcl-2 protein levels (6, 8).

Many of the elements that regulate mRNA stability are located in the 3'-untranslated region (3'-UTR) of the mRNA (for review, see Ref. 9). Prominent among these elements are the AU-rich elements (AREs), which are found in numerous short-lived cytokine and oncogene mRNAs. AREs increase the rate of poly(A) shortening as well as the rate of subsequent decay of the mRNA body (10, 11). AREs also appear to increase the rate of decapping of mRNA (12). Cellular factors that interact with AREs have been found to modulate the stability of ARE-containing mRNAs *in vivo* in both positive and negative fashions. For example, HuR has been found to stabilize ARE-containing mRNAs (13, 14), whereas AUF1 (15) and tristetraproline (16–18) contribute to specific ARE mRNA destabilization. Although the mechanisms by which these proteins modulate the decay of ARE-RNAs is not fully understood, it has been reported that ARE-binding proteins recruit the exosome to ARE-mRNAs (19), thereby promoting rapid 3'-5' exonucleolytic decay (19, 20).

Schiavone *et al.* (7) reported that there is an ARE in the 3'-UTR of *bcl-2* mRNA that is a functional destabilizing element. Subsequently, Donnini *et al.* (21) found that UVC-induced apoptosis of Jurkat cells leads to decreased *bcl-2* mRNA levels accompanied by increased binding of a number of cytoplasmic proteins to a *bcl-2* ARE riboprobe. Recently it was found that UVC treatment of Jurkat cells leads to increased binding of the p45 isoform of AUF1 to ARE RNA (22), suggesting that AUF1 plays a role in *bcl-2* mRNA destabilization in those cells.

In other cells, less is known about the *cis*-acting elements or *trans*-acting factors that regulate *bcl-2* mRNA stability in response to apoptotic agents. We have recently reported that HL-60 cell extracts contain proteins that bind to the first ARE in *bcl-2* mRNA (ARE 1) (nucleotides 921–1057 of *bcl-2* cDNA (1)) and that these proteins are inactive or decreased in HL-60 cells treated with taxol or okadaic acid for 32 h (8). UV-induced RNA cross-linking assays revealed that HL-60 cell extracts contain ~8 proteins ranging in size from 32 to 100 kDa that bind to ARE 1 RNA *in vitro* (8). Interestingly, RNA cross-linking to ~70- and ~38-kDa proteins was dramatically reduced after 20 h of taxol or OA treatment, and cross-linking to 4 proteins of 45–60 kDa was progressively reduced with 10–34 h of OA or taxol treatment. Taken together these studies suggested that taxol- or OA-induced *bcl-2* mRNA destabilization in HL-60 cells involves inactivation of *trans*-acting factors, which stabilize *bcl-2* mRNA through interaction with at least one of the four AU-rich elements present in the 3'-UTR of *bcl-2* mRNA. Although these earlier studies ruled out the participation of the mRNA-stabilizing protein HuR in the formation of HL-60 protein-ARE complexes, the identity of the proteins that bind to *bcl-2* ARE 1 remained unknown. Accordingly, to shed

\* This work was supported in part by development funds awarded to the Hollings Cancer Center by the United States Department of Defense and by Public Health Service Grant CA 87553 (NCI, National Institutes of Health) (to E. K. S.). The costs of publication of this article were defrayed in part by the payment of page charges. This article must therefore be hereby marked "advertisement" in accordance with 18 U.S.C. Section 1734 solely to indicate this fact.

§ These authors contributed equally to this study.

|| To whom correspondence should be addressed: Dept. of Biochemistry and Molecular Biology, Medical University of South Carolina, P. O. Box 250509, Charleston, SC 29425. Tel.: 843-792-7475; Fax: 843-792-8565; E-mail: spicer@musc.edu.

<sup>1</sup> The abbreviations used are: OA, okadaic acid; UTR, untranslated region; ARE, AU-rich element; taxol, paclitaxel; CAT, chloramphenicol acetyltransferase.

light on the mechanisms of taxol- and OA-induced apoptosis, we identified *bcl-2* ARE 1-binding proteins from HL-60 cells that are responsive to taxol and OA treatment. We also examined the effect of one of the ARE-binding proteins on ARE mRNA stability in cell extracts to determine its potential as a modulator of *bcl-2* mRNA stability *in vivo*.

#### EXPERIMENTAL PROCEDURES

**Cell Culture**—Human HL-60 leukemia cells (ATCC) were grown in RPMI 1640 medium (Invitrogen) supplemented with 10% (v/v) heat-inactivated fetal bovine serum, 100 units/ml penicillin, and 100  $\mu$ g/ml streptomycin. Cells were maintained at 37 °C in 95% air, 5% CO<sub>2</sub> in a fully humidified incubator. Cells were treated with taxol (200 nM) or okadaic acid (20 nM) as previously described (8).

**Preparation of Cell Extracts**—For protein purification HL-60 cells ( $2 \times 10^8$ ) were harvested by centrifugation at  $100 \times g$  for 5 min at 4 °C. The cells were washed twice with phosphate-buffered saline and suspended in 50 ml of buffer A (50 mM Tris-HCl, pH 7.5, 150 mM NaCl, 0.1% protease inhibitor mixture (Sigma) containing 104 mM 4-[2-aminoethyl]-benzenesulfonyl fluoride, 0.08 mM aprotinin, 2.1 mM leupeptin, 3.6 mM bestatin, 1.5 mM pepstatin, and 1.5 mM E-64. Cells were lysed with three 10-s bursts using a Virsonic Sonicator (Virtis) and subjected to low speed centrifugation ( $10,000 \times g$ ) for 10 min followed by centrifugation at  $100,000 \times g$  for 1 h at 4 °C to produce an S100 extract.

HL-60 S100 extracts for RNA decay assays were prepared from  $2 \times 10^6$  cells. Untreated cells or cells treated with 20 mM OA for 24 h were washed twice with phosphate-buffered saline, suspended in 200  $\mu$ l of buffer D (10 mM HEPES, pH 8.0, 3.0 mM MgCl<sub>2</sub>, 40 mM KCl, 0.1% protease inhibitor mixture, 0.2% Nonidet P-40, 10% glycerol, 1 mM dithiothreitol), and incubated on ice for 10 min. The lysate was centrifuged at  $10,000 \times g$  for 2 min followed by centrifugation at  $100,000 \times g$  for 1 h at 4 °C. Samples were stored in aliquots at -80 °C after flash-freezing on dry ice.

**Heparin-Sepharose Column Chromatography**—A 5-ml Hi-Trap™ heparin-Sepharose column (Amersham Biosciences) was equilibrated with 50 ml of start buffer (50 mM Tris-HCl, pH 7.5, 100 mM NaCl, 10% glycerol, 0.2 mM EDTA, 0.5 mM dithiothreitol and 1 mM 4-[2-aminoethyl]-benzenesulfonyl fluoride). Thirty ml of S-100 extract dialyzed against start buffer were loaded onto the pre-equilibrated column with a peristaltic pump at a rate of ~0.5 ml/min. The column was washed with 15 ml of start buffer, and bound proteins were eluted with a 50-ml linear gradient of 0–1.0 M NaCl in start buffer (0.5 ml/min flow rate). One-ml fractions were collected and monitored for absorbance at 280 nm. Selected fractions were desalted and concentrated using a Microcon concentrator (Millipore). All procedures were performed at 4 °C.

**Preparation of RNA Transcripts**—ARE 1,  $\beta$ -globin, CAT, and  $\alpha$ -operon RNA transcripts were synthesized using T7 RNA polymerase from pCR4-ARE 1, pCR4- $\beta$ -globin, pCR4-CAT (8), and  $\alpha$ -operon (23) plasmids, respectively. <sup>32</sup>P-Labeled RNAs were synthesized in transcription reactions containing 40  $\mu$ Ci of [<sup>32</sup>P]uridine triphosphate (Amersham Biosciences). To maximize the amount of full-length product reactions contained 250  $\mu$ M unlabeled UTP along with 500  $\mu$ M each ATP, CTP, and GTP. The purity of [<sup>32</sup>P]RNA transcripts was monitored by analysis on 6% polyacrylamide, 7 M urea gels, and the amounts of full-length products were  $\geq 90\%$ . Transcripts containing (AUUU)<sub>5</sub>A were prepared from a derivative of plasmid pSP70 (24) (a gift from B. Tholanikunnel, Medical University of South Carolina) using SP6 RNA polymerase.

**RNA Gel Mobility Shift Assays**—RNA mobility shift assays were performed as described previously (8). Briefly, column fractions (5  $\mu$ l) or purified protein (2–7.5  $\mu$ g) were mixed with [<sup>32</sup>P]RNA transcripts (20,000 cpm) in 20  $\mu$ l of RNA binding buffer (8) and incubated on ice for 10 min. Samples were analyzed on a 1% agarose, Tris acetate-EDTA gel, which was electrophoresed at 4 °C, dried on nitrocellulose paper, and analyzed by phosphorimaging using a STORM™ PhosphorImager and Image Quant™ software (Molecular Dynamics). For antibody supershift assays, column fractions were incubated with 50  $\mu$ g/ml monoclonal anti-human nucleolin antibody (Santa Cruz) for 10 min at room temperature before incubation with [<sup>32</sup>P]RNA. For competition assays,  $10 \times$  (~90 nM) or  $25 \times$  (225 nM) concentrations of homologous RNA (unlabeled ARE 1) or non-homologous RNA were added to samples containing 9 nM <sup>32</sup>P-ARE 1 RNA before the addition of purified recombinant nucleolin. Non-homologous RNAs included a 224-nucleotide  $\beta$ -globin transcript, a 284-nucleotide CAT transcript, and a 112-nucleotide  $\alpha$ -operon transcript. RNA concentrations were determined by absorbance at 260 nm.

**UV Cross-linking**—Five  $\mu$ l of <sup>32</sup>P-ARE 1 RNA transcript ( $2 \times 10^5$

cpm) were incubated with 10  $\mu$ l of concentrated column fractions in binding buffer at 4 °C for 10 min. Reaction mixtures were then transferred to a 96-well microtiter plate and exposed to 254 nm UV irradiation at a distance of 7 cm for 30 min on ice using a mineral light lamp (model UVG-54, Ultraviolet, Inc.). After UV-cross-linking, reactions were treated with RNase A (0.15 units/ $\mu$ l) and RNase T1 (60 units/ $\mu$ l) at 37 °C for 30 min. Samples were separated on a 12% polyacrylamide-SDS gel, which was then stained with Coomassie Brilliant Blue R-250 (Bio-Rad), dried, and exposed to a phosphor screen. RNA-cross-linked protein bands were visualized by phosphorimaging of the dried gels. Molecular mass markers were visualized with radioactive ink.

***bcl-2* ARE 1 RNA Affinity Column Chromatography**—*In vitro* transcribed *bcl-2* ARE 1 RNA was biotinylated using Photoprobe™ biotin (Vector Laboratories) according to the manufacturer's recommendations. In brief, 250  $\mu$ l of *bcl-2* ARE 1 RNA (0.5  $\mu$ g/ $\mu$ l) were mixed with 250  $\mu$ l of biotin and exposed to 365-nm UV light for 30 min to covalently couple biotin to the RNA. After biotinylation, 500  $\mu$ l of 0.1 M Tris/HCl, pH 9.5 were added to the coupling reaction. Unincorporated biotin was removed by extracting the mixture twice with 1.0 ml of 2-butanol. Biotinylated RNA (~250  $\mu$ l) was precipitated by the addition of 62.5  $\mu$ l of 10 M ammonium acetate, 12.5  $\mu$ l of 1 M MgCl<sub>2</sub>, and 625  $\mu$ l of 95% ethanol. After centrifugation the RNA pellet was washed with 70% ethanol and dissolved in 250  $\mu$ l of buffer B (50 mM Tris-HCl, pH 7.5, 100 mM NaCl, 0.1% protease inhibitor mixture). Before mixing with the biotin-RNA, heparin-Sepharose column fractions were dialyzed against buffer B and concentrated ~6-fold. The protein sample (250  $\mu$ l) was then incubated with 250  $\mu$ l of the biotin-ARE-RNA for 1 h at 4 °C with gentle shaking. To recover the RNA, 300  $\mu$ l of Vectrex Avidin D (Vector Laboratories) was added to the protein-RNA mixture. After incubation for 1 h at 4 °C the samples were centrifuged at  $10,000 \times g$  in a microcentrifuge for 30 s, and the matrix pellet was washed with 10 column volumes of buffer B. Proteins were eluted from the matrix with a step gradient of NaCl (0.2 to 1.0 M in 0.2 M steps) in 0.2 ml of buffer B.

**Mass Spectroscopy**—Samples eluted from the RNA affinity column were separated on a 12% polyacrylamide, 0.1% SDS gel. The gel was stained with Coomassie Blue, and individual bands corresponding to RNA-cross-linked proteins were excised from the gel. Gel slices were destained twice in 750  $\mu$ l of 1:1 (v/v) 100 mM ammonium bicarbonate, pH 8.0/methanol for 30 min. Gel bands were then washed with 750  $\mu$ l of 100 mM ammonium bicarbonate followed by washing with 750  $\mu$ l of 1:1 (v/v) 10 mM ammonium bicarbonate/acetonitrile for 15 min. Dehydration was accomplished with 500  $\mu$ l of acetonitrile for 15 min. The acetonitrile was removed, and the gel slices were dried in a SpeedVac. Proteins were digested with 100 ng of trypsin in 100 mM ammonium bicarbonate at 37 °C for 18 h. The supernatant was removed, and tryptic peptides were extracted with 50  $\mu$ l of 50% acetonitrile, 5% formic acid and bath-sonicated for 20 min. The supernatant was again removed and added to the original supernatant. Further extraction was accomplished by the addition of 50  $\mu$ l of 95% acetonitrile, 5% formic acid and sonication for 20 min. The combined extracts were dried in a SpeedVac. Peptides were reconstituted in 10% acetonitrile, 0.1% trifluoroacetic acid and desalted using a C18 ZipTip™ (Millipore). The peptides were eluted in 3  $\mu$ l of 49% acetonitrile, 49% deionized water, 2% acetic acid.

For matrix-assisted laser desorption ionization (MALDI) analysis, 0.5  $\mu$ l of desalted peptides was mixed with 1.5  $\mu$ l of  $\alpha$ -cyano-4-hydroxycinnamic acid matrix (50 mM, 50% acetonitrile), and 0.5  $\mu$ l of this was spotted onto a MALDI plate. MALDI mass spectra were acquired with a Voyager-DE instrument (Applied Biosystems). Typically, spectra from 250 laser shots were averaged to produce a MALDI mass spectrum. Peptide sequencing was accomplished by tandem mass spectrometry on an LCQ Classic ion trap mass spectrometer (Finnigan). Desalted peptides were ionized via a custom nanospray source. Peptides of interest were selected according to their *m/z* ratios and fragmented to produce sequence informative fragmentation patterns. Short stretches of sequence interpreted from tandem mass spectra, termed sequence tags, were searched against the NCBI non-redundant protein data base via the internet algorithm PepSea ([www.umb.br/cbsp/paginiciais/pepseaseqtag.htm](http://www.umb.br/cbsp/paginiciais/pepseaseqtag.htm)).

**Western Blot**—Protein concentrations in cell extracts were estimated by Bradford assay (Bio-Rad) using bovine serum albumin as a standard. Equal amounts of protein (40  $\mu$ g) were boiled in denaturation buffer for 5 min and separated on a 12% polyacrylamide, SDS gel. The proteins were electroblotted to Immobilon-P membrane (Millipore). To confirm that equal amounts of protein were present in the samples, a duplicate gel was run that was stained with Coomassie Blue. The polyvinylidene difluoride membrane was blocked by overnight incubation in 5% nonfat dry milk in TBS-T buffer (10 mM Tris-HCl, pH 8.0, 150 mM NaCl, 0.05% Tween 20) at 4 °C. The membrane was then incubated at room temper-

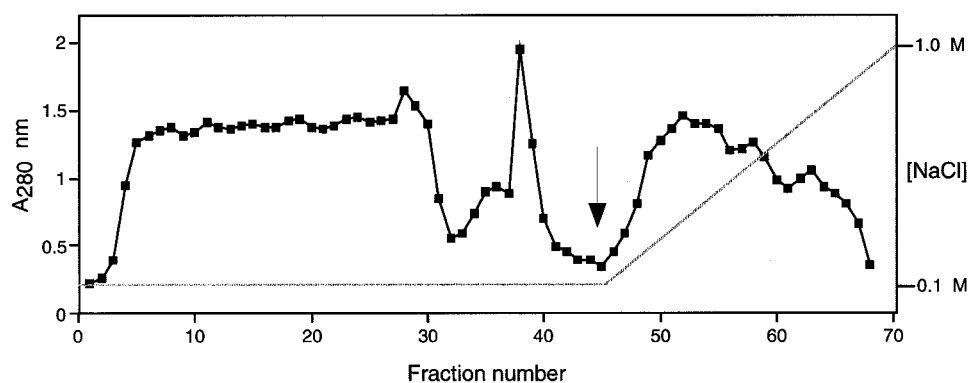


FIG. 1. **Chromatography of HL-60 S100 extracts on heparin-Sepharose.** S100 extracts were applied to a heparin-Sepharose column equilibrated in start buffer. Fractions 1–32 were flow-through fractions. After column washing (fractions 33–45), bound proteins were eluted with a linear gradient of 0.1–1.0 mM NaCl (fractions 46–68). Absorbance at 280 nm is plotted versus fraction number; the arrow indicates the start of the salt gradient (indicated by the grey line).

ature for 1 h with anti-human-nucleolin (C-23) monoclonal antibody (0.2  $\mu\text{g}/\text{ml}$ ) and anti- $\beta$ -actin polyclonal antibody (0.2  $\mu\text{g}/\text{ml}$ ) (Santa-Cruz Biotechnology) in fresh blocking buffer. Unbound antibody was removed by four 10-min washes in TBS-T buffer. The membrane was then incubated with horseradish peroxidase-conjugated goat-anti-mouse secondary antibody (0.2  $\mu\text{g}/\text{ml}$ ) (Santa-Cruz) for 1 h at room temperature followed by four 10-min washes with TBS-T. The blot was then developed with luminol reagent (Santa-Cruz). Cruz markers (Santa-Cruz) were used as internal molecular weight standards.

**Expression and Purification of Recombinant Nucleolin**—A recombinant pET21a plasmid carrying a truncated nucleolin gene encoding residues 284–707 and six histidines (25) was a gift from Dr. France Carrier (University of Maryland). *Escherichia coli* BL21 cells transformed with pET- $\Delta\text{Nuc-His}$  were grown until the  $A_{600} = 0.6$  and then induced overnight with 0.4 mM isopropyl-1-thio- $\beta$ -D-galactopyranoside at 30  $^{\circ}\text{C}$ . After induction cell pellets were resuspended in buffer C (20 mM sodium phosphate buffer (pH 7.4), 500 mM NaCl, 10 mM imidazole, 1 mM phenylmethylsulfonyl fluoride) and lysed by sonication. The lysate was centrifuged at 12,000  $\times g$  for 30 min. The supernatant was loaded onto a 1.7-ml metal chelate (POROS MC-M) column (BioCAD SPRINT perfusion chromatography system) equilibrated with buffer C. After washing with buffer C,  $\Delta\text{Nuc-His}$  was eluted with a linear gradient of 0–200 mM imidazole in buffer C. Imidazole was removed by dialysis, and the protein was concentrated using a Microcon concentrator. Protein purity was assessed by SDS-PAGE, and protein concentration was measured by Bradford assays.

**In Vitro mRNA Decay Assays**—A 248-nucleotide region of the  $\beta$ -globin gene and a 384-nucleotide  $\beta$ -globin-ARE fusion gene were subcloned from pBBB4 (26) and pBBB-ARE (8), respectively, into the pCR4 Topo-TA vector. In addition, reverse transcription-PCR fragments containing a portion of the *bcl-2*-coding region (nucleotides 600–750) or coding region plus ARE (nucleotides 600–1057) were cloned into pCR4. Spe-I linearized pCR4- $\beta$ -globin, pCR4- $\beta$ -globin-ARE, pCR4-*bcl*-CR, and pCR4-*bcl*-CR ARE plasmids were used as templates for synthesis of  $\beta$ -globin,  $\beta$ -globin-ARE, *bcl-2* coding region, and *bcl-2*-coding region ARE transcripts, respectively. 5'-Capped  $^{32}\text{P}$ -labeled transcripts were prepared using a mMessage mMachine T7 kit (Ambion), following the manufacturer's instructions. Poly(A) tails of  $\sim 150$  nucleotides were added to the 3'-ends of the transcripts using a poly(A) tailing kit (Ambion), and unincorporated NTPs were removed by G-25 spin column chromatography. Approximately 150,000 cpm of capped and polyadenylated  $\beta$ -globin-ARE and  $\beta$ -globin RNAs were used per decay reaction, which was performed as described by Ford and Wilusz (27). Typically, a 70- $\mu\text{l}$  reaction mixture contained 16  $\mu\text{l}$  of 10% polyvinyl alcohol, 5  $\mu\text{l}$  of a 12.5 mM ATP and 250 mM phosphocreatine mixture, 5  $\mu\text{l}$  of 500 ng/ $\mu\text{l}$  poly(A) (Amersham Biosciences), 5  $\mu\text{l}$  of  $^{32}\text{P}$ -labeled transcript ( $\sim 175$  nM), and 8.8  $\mu\text{g}$  of protein in HL-60 S100 extract. To assay the affect of nucleolin on RNA decay, purified  $\Delta\text{Nuc-His}$  (280 nM final concentration) was added to RNA decay reactions before the addition of cell extracts. Samples were incubated at 30  $^{\circ}\text{C}$ , and the reaction was stopped at various times by transferring 14.5- $\mu\text{l}$  aliquots to 100  $\mu\text{l}$  of stop buffer (400 mM NaCl, 25 mM Tris-HCl, pH 7.5, 0.1% SDS) and immediately extracting with 100  $\mu\text{l}$  of phenol-chloroform. RNA was ethanol-precipitated and then electrophoresed on 6% polyacrylamide gels containing 7 M urea (27). After electrophoresis, gels were fixed, dried, and analyzed by phosphorimaging.

## RESULTS

**Purification of Proteins That Bind to *bcl-2* ARE 1**—To purify *bcl-2* ARE-binding proteins, HL-60 cell extracts were subjected to heparin-Sepharose chromatography followed by ARE RNA affinity chromatography. In the first purification step, HL-60 S100 extracts were applied to a heparin-Sepharose column equilibrated with start buffer. Proteins were eluted from the column with a linear gradient of 0–1.0 M NaCl. As shown in Fig. 1, proteins were eluted across the entire salt gradient. Fractions eluted from the column were assayed for protein content (Fig. 2A) and tested for ARE 1 binding by UV-induced RNA-cross-linking (Fig. 2B) and RNA gel mobility shift assays (Fig. 2C). As shown in Fig. 2, fractions 51, 53, 55, and 58 contained proteins that bind to ARE 1 in both assays. In the UV-cross-linking assays the predominant cross-linked proteins were in the 40–60-kDa molecular mass range in the total protein extracts, whereas in heparin column fraction 58, the most efficiently cross-linked proteins were 70 and 100 kDa. This presumably reflects differences in the abundance of these proteins in the different samples. Fractions 57–59 were pooled and selected for further purification because these fractions contained an  $\sim 70$ -kDa protein that potentially corresponds to the 70-kDa protein observed to be responsive to taxol and OA treatment (8). Additionally, these fractions contained proteins that exhibited efficient RNA cross-linking and consisted of the least complex mixture of proteins (Fig. 2A).

To further purify the ARE-binding proteins, fractions 57–59 were subjected to ARE RNA affinity chromatography. An ARE RNA affinity matrix was prepared by coupling ARE 1 RNA synthesized by *in vitro* transcription to biotin using Photoprobe<sup>TM</sup> biotin. The biotinylated ARE RNA was incubated with pooled fractions 57–59 in RNA binding buffer and then incubated with avidin D-Vectrex matrix. After extensive washing of the RNA-biotin-avidin matrix, bound proteins were eluted with a 0.2 M step gradient of 0.2–1.2 M NaCl in buffer B. SDS-PAGE analysis of the eluted proteins (Fig. 3A) indicated that the majority of the proteins in the pooled heparin fractions did not bind to the ARE RNA matrix (compare lanes S and FT). However, the first three salt-eluted fractions contained a small number of proteins including three prominent bands of  $\sim 100$ ,  $\sim 70$ , and 32 kDa. The 100-kDa protein was significantly enriched relative to its concentration in the sample applied to the column (Fig. 3A).

Fractions eluted from the RNA matrix were desalted and analyzed by UV cross-linking and gel shift assays. As shown in Fig. 3B, the 0.2, 0.4, and 0.6 M NaCl fractions contained proteins of  $\sim 100$ , 70, and 50 kDa that UV-cross-link to ARE-RNA.

**FIG. 2. UV cross-linking and RNA binding assays of heparin-Sepharose column fractions.** Selected column fractions were desalted and subjected to UV cross-linking and gel shift assays. *A* and *B*, 10- $\mu$ l aliquots of the indicated fractions were incubated with  $^{32}$ P-ARE 1 RNA in RNA binding buffer and exposed to UV light (254 nm) for 30 min. Complexes were digested with RNase A and T1, and proteins were separated by SDS-PAGE. *MW*, molecular weight markers. *A*, image of the Coomassie Blue-stained gel. *B*, phosphorimage of the SDS gel detected on a STORM imager. *S*, sample. *C*, gel shift assay. Indicated fractions were incubated with  $^{32}$ P-ARE 1 RNA in RNA binding buffer. Free and complexed RNAs were separated by electrophoresis on a 1% agarose gel, which was dried and analyzed by phosphorimaging, as in *B*.

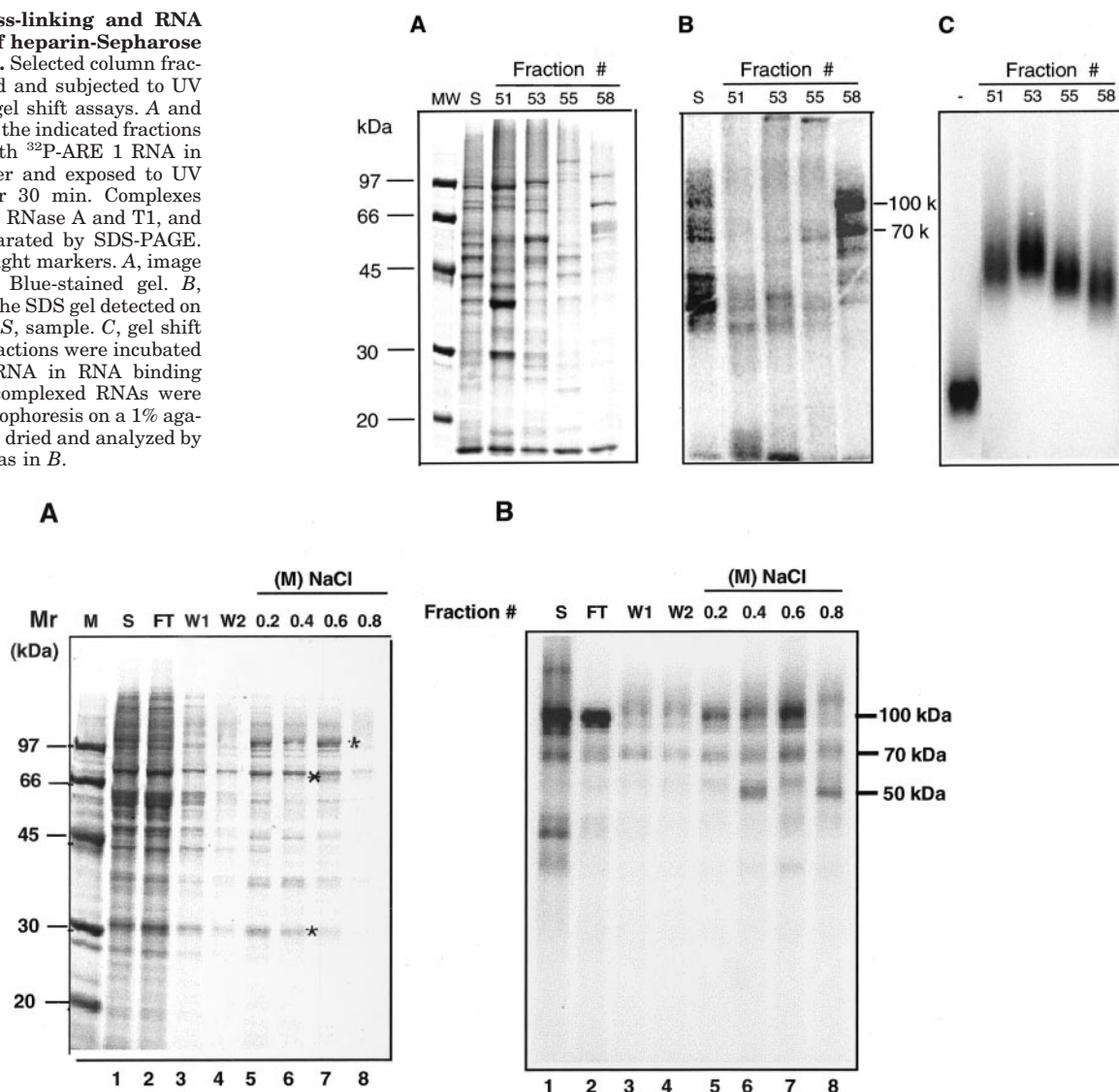


**FIG. 3. RNA affinity purification of heparin column fractions.** Heparin-Sepharose fractions 57–59 were pooled and incubated with biotinylated ARE 1 RNA. The sample was then incubated with avidin D-Vectrex, and bound proteins were eluted with a step gradient of 0.2–1.0 M NaCl in buffer B. Aliquots of the eluted fractions were assayed for binding to *bcl-2* ARE 1 by UV cross-linking as in Fig. 2. After UV treatment, proteins were separated by SDS-PAGE, and the gel was stained with Coomassie Blue (*A*) and exposed to a phosphorimage plate (*B*). In *panel A*, *M* indicates molecular weight markers. *Panels A* and *B*, lane 1, sample (*S*) applied to column; lane 2, flow-through (*FT*); lanes 3 and 4, wash (*W*) fractions; lanes 5–8, fractions eluted with 0.2, 0.4, 0.6, and 0.8 M NaCl, respectively. The asterisks indicate bands excised from the gel for MALDI-MS analysis.

All four salt-eluted fractions also produced a shift in the electrophoretic mobility of ARE 1 RNA (Fig. 4A). Proteins in these fractions exhibited specificity for ARE 1 RNA, as they did not bind to a 40-nucleotide RNA transcript containing a repeat of the AUUUA pentamer ((AUUU)<sub>5</sub>A) (Fig. 4B). The different sizes of the ribonucleoprotein complexes (Fig. 4A) presumably are due to binding of more than 1 protein to the 220-nucleotide probe RNA (e.g. different combinations of the 50-, 70-, and 100-kDa proteins may be present in the ribonucleoprotein complexes).

**Identification of the 100-, 70-, and 32-kDa Proteins**—The 100-, 70-, and 32-kDa bands were selected for further analysis because SDS-PAGE indicated they were enriched in the affinity matrix fractions and they were among the most abundant proteins in the eluted fractions (Fig. 3). Additionally, the 100- and 70-kDa proteins were efficiently cross-linked to ARE RNA (Figs. 2 and 3). The 50-kDa band was not examined further because it was present in lower abundance and was not well separated from other protein bands on the SDS gel. To determine the identity of the selected proteins, the corresponding

bands in the 0.4 and 0.6 M NaCl fractions were excised from the Coomassie Blue-stained SDS-polyacrylamide gel (Fig. 3A) and subjected to MALDI-mass spectrometry (MS) analysis. This analysis included in-gel digestion with trypsin followed by MALDI-MS analysis of peptides eluted from each gel slice. Two peptides from the 100-kDa protein were selected for sequencing by tandem mass spectrometry. Comparison of the sequences of the two peptides with the sequence of peptides in the NCBI protein data base using the program BLAST (28) indicated that the two peptides match amino acids 611–624 and 349–352, respectively, of human nucleolin. The mass/charge ratio (*m/z*) of seven additional peptides in the MALDI mass spectrum matched those of nucleolin. Other peaks in the spectrum were identified as peptides from trypsin or a MALDI mass standard, but no other non-nucleolin peptides were identified. Similar MALDI-MS analysis of the 70- and 32-kDa proteins revealed the presence of peptides that match the mass of nucleolin peptides, indicating they both are proteolytic fragments of nucleolin.

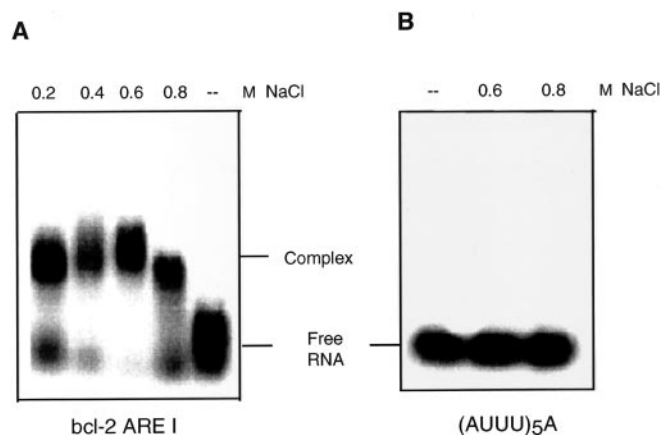


**FIG. 4. RNA binding activity of affinity matrix fractions.** Aliquots of fractions eluted from the ARE 1 affinity column (Fig. 3) were incubated with  $^{32}\text{P}$ -RNA transcripts in binding buffer. RNA-protein complexes were electrophoresed on a 1% agarose-Tris acetate-EDTA gel. *A*, fractions eluted with 0.2, 0.4, 0.6, and 0.8 M NaCl, respectively, were incubated with a 200-nucleotide  $^{32}\text{P}$ -labeled ARE 1 transcript. *B*, fractions eluted with 0.4 and 0.6 M NaCl, respectively, were incubated with a  $^{32}\text{P}$ -labeled transcript containing the sequence (AUUU)<sub>5</sub>A.

**Binding of Nucleolin to ARE 1 in Vitro**—Gel shift assays indicated that proteins eluted from the ARE affinity matrix form complexes with ARE RNA but do not bind to (AUUU)<sub>5</sub>A RNA. However, these column fractions contained a number of proteins, only some of which may bind to ARE RNA. To confirm that nucleolin is one of the proteins present in the observed ARE-protein complexes (Fig. 4A), a gel mobility supershift assay was performed using anti-nucleolin antibody. As shown in Fig. 5, incubation of  $^{32}\text{P}$ -ARE RNA with pooled aliquots of the 0.4 and 0.6 M NaCl fractions from the ARE 1 affinity column produced a shift in the RNA mobility (Fig. 5, lane 2). When ARE RNA and the pooled fractions were incubated in the presence of anti-human-nucleolin monoclonal antibody, a supershifted protein-RNA-antibody complex was observed (Fig. 5, lane 3). Thus, nucleolin is present in the protein-RNA complexes formed with the affinity column fractions. Whether the 100- and/or 70-kDa forms of nucleolin are present in the protein-RNA complexes remains unknown. Also, it is not known if the 50-kDa protein detected in the UV-cross-linking assay (Fig. 3) is a fragment of nucleolin. The partial supershift seen with anti-nucleolin antibody suggests additional proteins may be present in the protein-RNA complexes (Fig. 5).

The UV cross-linking assays suggest that nucleolin binds directly to ARE RNA rather than binding to another protein that is bound to ARE RNA. To confirm this, the ARE RNA binding activity of purified recombinant nucleolin was tested. A fragment of human nucleolin containing a (His)<sub>6</sub> tag encoded on pET21a-Nuc (25) was expressed in *E. coli* and purified by Ni<sup>2+</sup> column chromatography. This recombinant nucleolin ( $\Delta\text{Nuc-His}$ ), which contains amino acids 284–707, contains the RNA binding domain of nucleolin (residues 284–629) and retains its RNA binding activity (29). As shown in Fig. 6, incubation of  $\Delta\text{Nuc-His}$  with ARE RNA resulted in formation of a protein-RNA complex in a gel shift assay. Thus, recombinant nucleolin can bind ARE RNA in the absence of other HL-60 proteins.

To examine the specificity of nucleolin binding to RNA, homologous or heterologous RNAs were added as competitors in RNA gel shift assays. In the presence of a 10-fold molar excess of unlabeled ARE RNA, the apparent size of nucleolin  $^{32}\text{P}$ -ARE RNA complexes was reduced, and no probe RNA was bound in the presence of a 25-fold excess of ARE RNA (Fig. 6). In contrast, the addition of the same concentration of  $\beta$ -globin, CAT, or  $\alpha$ -operon RNA transcripts did not inhibit the formation of

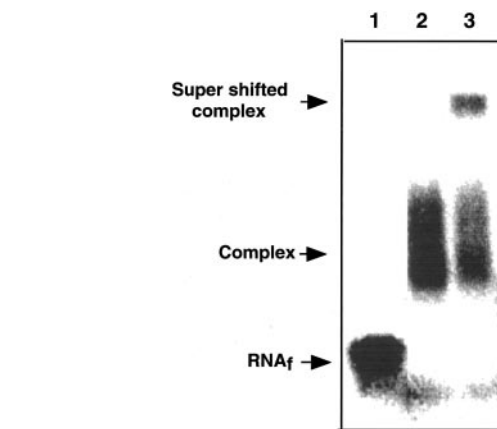


**FIG. 5. Nucleolin antibody supershift assay of affinity column fractions.** Aliquots of affinity column fractions eluted with 0.4 and 0.6 M NaCl were pooled and incubated with  $^{32}\text{P}$ -labeled *bcl-2* ARE 1 RNA in binding buffer for 10 min at 4 °C. Anti-nucleolin antibody (lane 3) or buffer (lane 2) was then added to the reaction mixture, and the samples were incubated for 25 min at room temperature. Free (RNA<sub>f</sub>) and complexed RNAs were separated on a 1% agarose-Tris acetate-EDTA gel, which was analyzed by phosphorimaging.

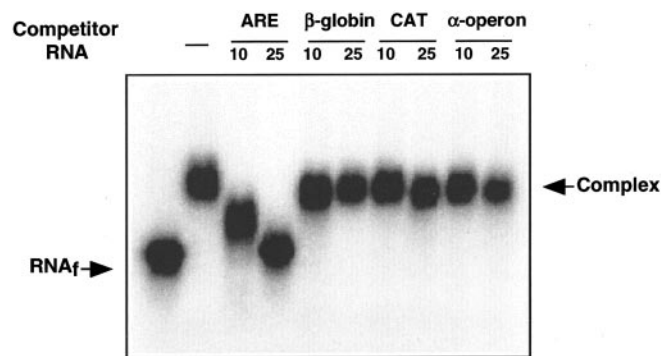


**FIG. 6. RNA binding specificity of recombinant nucleolin.** Recombinant nucleolin ( $\Delta\text{Nuc-His}$ ) was incubated with  $^{32}\text{P}$ -labeled *bcl-2* ARE 1 RNA in the presence or absence of a 10 $\times$  or 25 $\times$  molar excess of unlabeled competitor RNAs as indicated. After incubation in RNA binding buffer, samples were separated on a 1% agarose-Tris acetate-EDTA gel, which was dried and analyzed by phosphorimaging. RNA<sub>f</sub>, free RNA.

nucleolin-ARE RNA complexes, as indicated by the absence of free  $^{32}\text{P}$ -ARE RNA in the gel shift assay (Fig. 6). Thus, recombinant nucleolin exhibits a  $\geq 25$ -fold preference for ARE RNA over other mRNAs. The intermediate mobility of the protein-RNA complex observed in the presence of a 10-fold excess of unlabeled ARE RNA (Fig. 6) further suggests that nucleolin-ARE RNA complexes formed in the presence of excess nucleolin contain 2 or more nucleolin molecules.

**Effect of Taxol and OA on Nucleolin in HL-60 Cells**—As previously reported, treatment of HL-60 cells with taxol or OA reduces the *bcl-2* ARE RNA binding activity of cell extracts and leads to *bcl-2* mRNA destabilization (8). Results reported here indicate that nucleolin binds specifically to *bcl-2* ARE 1, suggesting it may be one of the proteins that plays a role in regulating *bcl-2* mRNA stability in HL-60 cells. This raises the question of whether taxol or OA treatment down-regulates or inactivates nucleolin and subsequently decreases binding to *bcl-2* mRNA. To address this question nucleolin levels were examined in drug-treated cells by Western blotting. As shown in Fig. 7, untreated HL-60 cells contain a major band corresponding to full-length nucleolin (apparent mass of 100 kDa) and a less intense nucleolin band of  $\sim 70$  kDa. In cells treated with taxol or OA, the full-length nucleolin band progressively

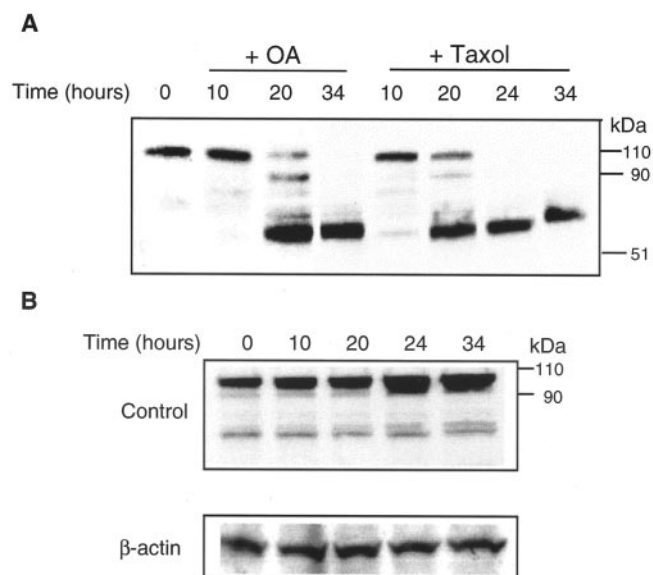


FIG. 7. Western blot analysis of nucleolin in HL60 cells treated with taxol or okadaic acid. *A*, extracts from cells treated for 0, 10, 20, or 34 h with 20 nM OA or with 200 nM taxol for 10, 20, 24, or 34 h (as indicated) were separated on a 12% polyacrylamide-SDS gel. After electrophoresis, proteins were transferred to Immobilon P paper and probed with monoclonal anti-human nucleolin antibody. *B*, untreated cells were harvested at 0, 10, 20, 24, and 34 h after dilution into fresh media, and extracts were probed with anti-nucleolin and anti- $\beta$ -actin antibodies, as indicated.

decreased and proteolytic fragments of 55–85 kDa increased during 10–34 h of drug treatment. Thus, nucleolin proteolysis occurred in a similar time frame as the changes in ARE RNA binding activity that have been observed upon taxol or OA treatment (8). In both untreated and treated cells the amount of nucleolin increased after 10–34 h of growth; however, in untreated cells there was no increase in proteolytic fragments of nucleolin (Fig. 7*B*).

**Nucleolin Stabilization of ARE mRNA *In Vitro***—To investigate the potential of nucleolin to stabilize *bcl-2* mRNA, RNA decay assays were performed using the *in vitro* assay system developed by Ford and Wilusz (27). Soluble cytoplasmic extracts (S100) were prepared from untreated and OA-treated HL-60 cells. Capped and polyadenylated mRNAs were used in these assays to mimic *in vivo* decay, which likely involves cap-stimulated deadenylation (30) by poly(A)-specific ribonuclease (31) followed by rapid decay of the mRNA body (27).  $^{32}$ P-Labeled  $\beta$ -globin,  $\beta$ -globin-ARE, *bcl-2*-coding region, and *bcl-2*-coding region-ARE transcripts were synthesized by *in vitro* transcription reactions in which the  $^7$ mGpppG cap was added co-transcriptionally. Poly(A) tails of ~150 nucleotides were subsequently added, and the mRNAs were incubated with S100 extracts in the presence of poly(A) (to activate deadenylation). At various times the reactions were stopped, RNA was isolated, and its recovery was analyzed by gel electrophoresis. As shown in Fig. 8,  $\beta$ -globin-ARE RNA decayed faster than  $\beta$ -globin RNA in untreated (control) HL-60 extracts. This is consistent with the more rapid decay of

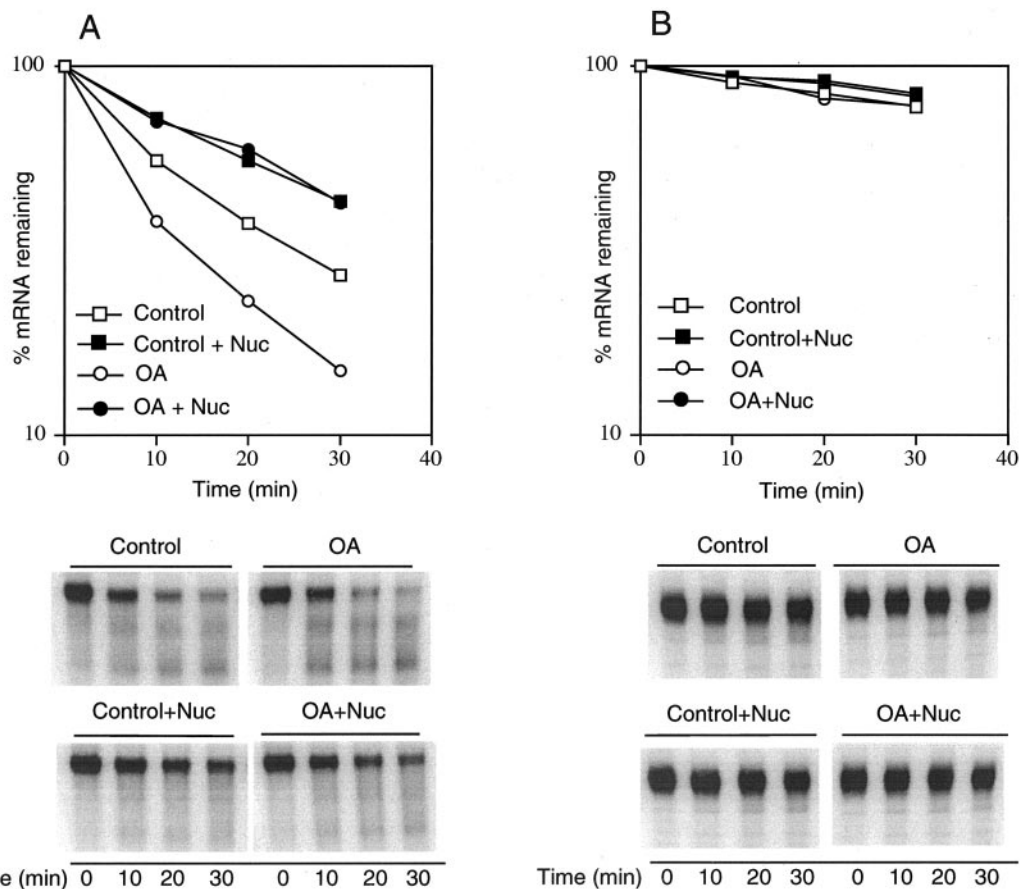


FIG. 8. Effect of nucleolin on decay of  $\beta$ -globin ARE mRNA in HL-60 extracts. *A*, decay of  $\beta$ -globin-ARE RNA in untreated (*Control*) or OA-treated HL-60 cell extracts. *Nuc*, nucleolin. *B*, decay of  $\beta$ -globin RNA in extracts of OA-treated or untreated HL-60 cells. The effect of nucleolin on decay of each mRNA was assessed by the addition of  $\Delta$ Nuc-His to control and OA-treated cell extracts before incubation with mRNAs. 5'-capped, polyadenylated  $^{32}$ P-labeled RNAs were incubated with S100 extracts and isolated at the indicated times. Extracts were prepared from untreated cells or cells treated for 24 h with OA (20 nM). RNA recovery was assessed by polyacrylamide gel electrophoresis and phosphorimaging. % RNA remaining indicates the amount of full-length mRNA recovered as a function of time of incubation in cell extracts. Data points are the average of two independent analyses; the maximum error range was  $\pm$  6%.

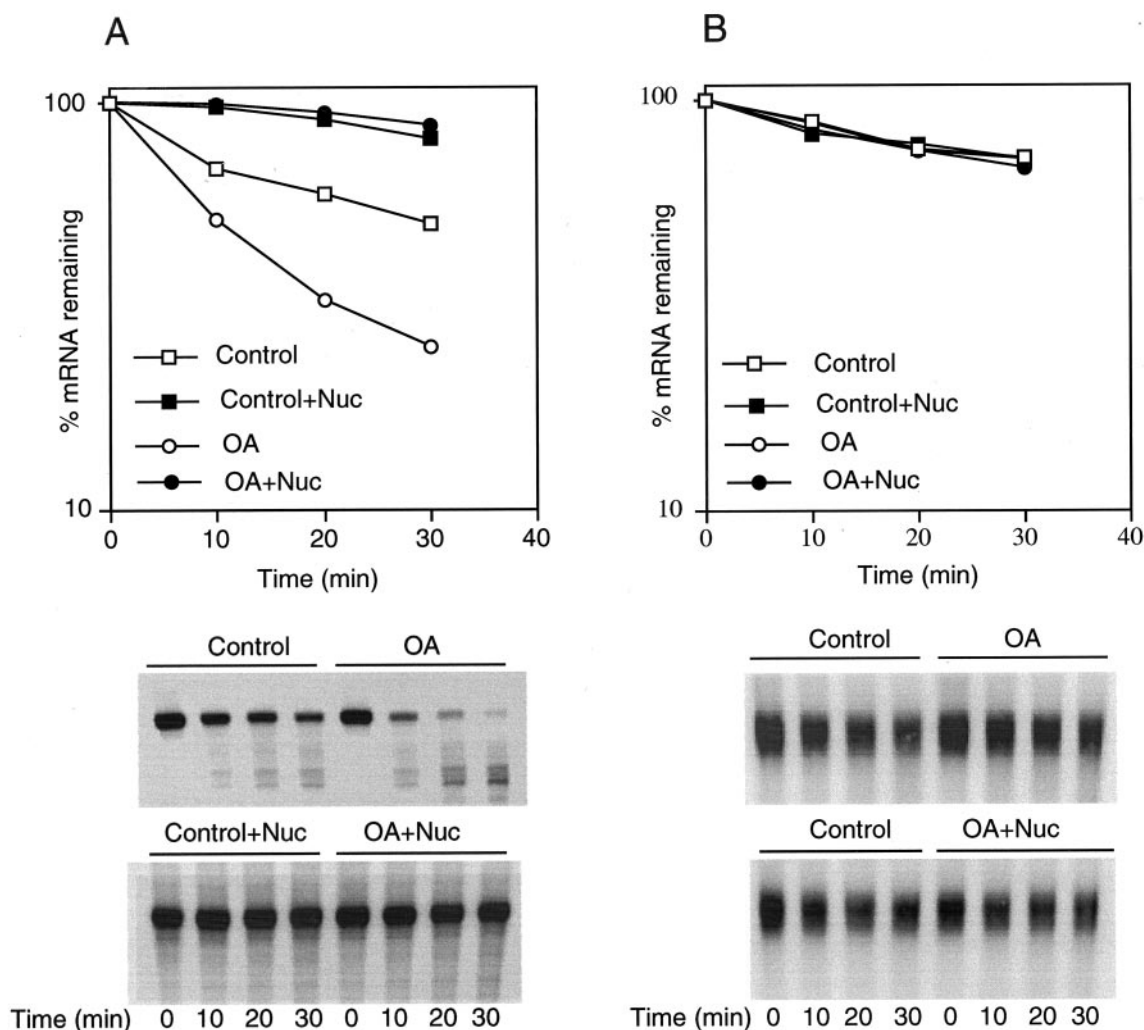


FIG. 9. Effect of nucleolin on decay of *bcl-2* ARE mRNA in HL-60 extracts. A, decay of *bcl-CR-ARE* RNA in untreated (Control) or OA-treated HL-60 cell extracts. Nuc, nucleolin. B, decay of *bcl-CR* RNA in extracts of OA-treated or untreated HL-60 cells. The effect of nucleolin on decay of each mRNA was assessed by the addition of  $\Delta$ Nuc-His to control and OA-treated cell extracts before incubation with mRNAs. Decay assays were performed as in Fig. 8. % RNA remaining indicates the amount of full-length mRNA recovered as a function of time of incubation in cell extracts. Data points are the average of two independent analyses; the maximum error range was  $\pm 5\%$ .

$\beta$ -globin-ARE RNA than  $\beta$ -globin RNA that was observed *in vivo* in transfected NIH 3T3 cells (8). Incubation of  $\beta$ -globin-ARE RNA in OA-treated S100 extracts resulted in more rapid decay than in extracts of untreated HL-60 cells (Fig. 8A). This decrease in stability is similar to the destabilization of *bcl-2* mRNA observed *in vivo* after OA treatment of HL-60 cells. In contrast,  $\beta$ -globin mRNA was equally stable in extracts of untreated and drug-treated cells (Fig. 8B). Similar results were observed with transcripts containing a portion of the *bcl-2*-coding region (*bcl-CR*) versus a transcript containing the *bcl-2*-coding region and the ARE (*bcl-CR-ARE*). *bcl-CR-ARE* decayed faster in untreated or OA-treated extracts (Fig. 9A) than *bcl-CR* transcripts (Fig. 9B). When purified recombinant nucleolin ( $\Delta$ Nuc-His) was added to extracts of OA-treated cells or to control extracts, both  $\beta$ -globin-ARE (Fig. 8A) and *bcl-CR-ARE* RNA (Fig. 9A) decayed at considerably slower rates. However, decay of  $\beta$ -globin and *bcl-CR* mRNAs (lacking ARE-1) in drug-treated extracts were not affected by the addition of nucleolin (Figs. 8B and 9B). Similar assays with capped, polyadenylated CAT mRNA (284 nucleotides) showed no effect of nucleolin on mRNA decay rates (data not shown). Thus, nucleolin increased the stability of mRNA in HL-60 cell extracts in an ARE-dependent manner.

#### DISCUSSION

Our previous studies indicated that HL-60 extracts contain ~8 proteins or polypeptides that bind to *bcl-2* ARE 1 RNA (8). Prominent among these was a 70-kDa protein that exhibited sharply reduced cross-linking after 10 h of taxol or OA treatment of HL-60 cells. These studies suggested that the 70-kDa protein and possibly others binds and stabilizes *bcl-2* mRNA in HL-60 cells. Furthermore, treatment with taxol or OA reduces this binding and leads to *bcl-2* mRNA destabilization.

In this study we have purified three polypeptides of 100, 70, and 32 kDa by ARE RNA affinity chromatography. MALDI-MS analysis indicated that the polypeptide with an apparent mass of 100 kDa is nucleolin (which has a calculated mass of 76 kDa) and that the 70 and 32 kDa polypeptides are proteolytic fragments of nucleolin. Both the 100 and 70 kDa forms of nucleolin cross-link to ARE 1 RNA, whereas the 32-kDa fragment did not cross-link. The presence of nucleolin in protein-ARE complexes formed with affinity column fractions was confirmed by RNA supershift assays with anti-nucleolin antibody. Gel shift assays further demonstrated that recombinant nucleolin ( $\Delta$ Nuc-His) binds ARE 1 RNA specifically. Western blots confirmed that nucleolin is highly expressed in HL-60 cells. Collectively, these results suggest that nucleolin plays a positive role in the reg-

ulation of *bcl-2* mRNA stability. Consistent with this we observed that taxol or OA treatment of HL-60 cells leads to proteolysis of nucleolin in a similar time frame as *bcl-2* mRNA down-regulation. Strong support for the concept that nucleolin stabilizes *bcl-2* mRNA in HL-60 cells comes from our finding that recombinant nucleolin decreases the decay rate of ARE-containing mRNAs in OA-treated HL-60 cell extracts.

Nucleolin is an abundant, multifunctional protein that exhibits an unusual range of activities, including DNA binding, RNA binding, and possibly DNA-RNA helix unwinding (for review, see Refs. 32 and 33). Nucleolin contains four RNA binding domains that are involved in recognition of a variety of RNAs. In addition to playing an essential role in pre-rRNA processing (34), nucleolin is thought to regulate ribosomal DNA transcription (35–37) and is a component of the transcription factor LR1 (38). Interestingly, nucleolin has also been found to play a role in regulation of the stability of interleukin 2 mRNA (39) and amyloid precursor protein mRNA (40). Nucleolin has also been observed to bind to human preprorenin mRNA (41) and to be a component of a fragile X mental retardation protein (FMRP)-associated messenger ribonucleoprotein (mRNP) particle (42). Stabilization of interleukin 2 mRNA in response to T-cell activation involves binding of nucleolin to a response element in the 5'-UTR of interleukin 2 mRNA. Nucleolin also has been shown to bind to a 29-nucleotide element in the 3'-UTR of amyloid precursor protein mRNA (43) and contribute to the stabilization of the mRNA (44). Interestingly, the predicted secondary structure of *bcl-2* ARE 1 contains a stem-loop with a sequence in the loop (UCCCA) that is similar to the loop sequence (UCCCGA) in the nucleolin recognition element in pre-rRNA (45). However, there is little sequence similarity between *bcl-2* ARE 1 and the 29-nucleotide element in amyloid precursor protein mRNA or the 22-nucleotide response element in interleukin 2 mRNA which are bound by nucleolin.

Previous observations that *bcl-2* mRNA is destabilized by treatment of HL-60 cells with OA, an inhibitor of protein phosphatases 1 and 2A (46), or taxol, which induces phosphorylation of c-Raf-1 and Bcl-2 proteins (47), suggested that *bcl-2* mRNA down-regulation may involve phosphorylation of a stabilizing *trans*-factor (8). Interestingly, nucleolin is a phosphoprotein that is highly expressed in proliferating cells (48). Nucleolin is a substrate for several kinases including protein kinase C (49), and there is evidence suggesting that nucleolin is a substrate for protein phosphatases (50, 51). Importantly, nucleolin is threonine-phosphorylated by p34<sup>cdc2</sup> kinase during mitosis (32, 33). Because taxol is a mitotic inhibitor (52), the accumulation of taxol-treated cells in M phase would be expected to increase the extent of nucleolin phosphorylation. Phosphorylation of nucleolin appears to enhance its auto-degradation and to regulate some of its disparate activities (for review, see Ref. 32).

Based on these reports we hypothesize that in proliferating cells nucleolin binds to and stabilizes *bcl-2* mRNA, leading to overexpression of Bcl-2 protein. When cells are treated with okadaic acid or taxol, nucleolin is phosphorylated and subsequently cleaved into fragments that no longer bind *bcl-2* mRNA. In the absence of nucleolin and possibly other stabilizing proteins, *bcl-2* mRNA is then rapidly degraded via an ARE-dependent decay mechanism. This hypothesis is further supported by the observation that treatment of human fibroblasts with okadaic acid leads to hyperphosphorylation of N60, a proteolytic fragment of nucleolin (53). A similar process likely occurs with taxol treatment, since taxol-induced *bcl-2* mRNA decay is blocked by the tyrosine kinase inhibitor genistein (5).

The genetic hallmark of follicular lymphoma is represented by a t(14:18) chromosomal translocation that moves the *bcl-2*

gene into close proximity to the IgH transcription enhancer (1). Although it is clear that transcription of the *bcl-2* gene is enhanced in follicular lymphoma, increased levels of Bcl-2 protein are often observed in other cancers where the t(14:18) translocation has not occurred, such as chronic lymphocytic leukemia, acute myeloid leukemia, multiple myeloma, and metastatic breast cancer (2, 3, 54). This raises the intriguing possibility that in these tumors increased *bcl-2* mRNA stability contributes more to the elevated levels of Bcl-2 protein than transcriptional alterations. Thus, deciphering the role of nucleolin in up-regulating the expression of the *bcl-2* gene may provide important leads into the molecular mechanisms of cancer development and progression.

In summary, this study has identified a novel mechanism by which a chemotherapeutic drug can induce apoptosis in cancer cells. This mechanism entails the drug-induced down-regulation of nucleolin, a protein involved in stabilization of *bcl-2* mRNA. It is possible that other anticancer drugs which inhibit cell proliferation or promote cellular differentiation may also induce apoptosis via nucleolin down-regulation. For example, induction of apoptosis in U937 leukemia cells is accompanied by notable decreases in the levels of nuclear and cytoplasmic nucleolin (55). Under these conditions less nucleolin would be available in the cytoplasm to stabilize *bcl-2* mRNA. The potential of nucleolin in having a broader role in cancer development and drug-induced apoptosis is currently under investigation.

**Acknowledgments**—We gratefully acknowledge the expert MALDI-MS analysis performed by Dr. Kevin Schey (Medical University of South Carolina MALDI facility). We thank Dr. France Carrier (University of Maryland) for the gift of plasmid pET21-Nuc and Dr. Baby Tholanikunnel (Medical University of South Carolina) for the gift of plasmid pSP70-(AUU)<sub>5</sub>A.

#### REFERENCES

- Cleary, M. L., Smith, S. D., and Sklar, J. (1986) *Cell* **47**, 19–28
- Steube, K. G., Jadau, A., Teepe, D., and Drexler, H. G. (1995) *Leukemia (Baltimore)* **9**, 1841–1845
- Reed, J. C. (1997) *Adv. Pharmacol.* **41**, 501–532
- Gao, G., and Dou, Q.-P. (2000) *Mol. Pharmacol.* **58**, 1001–1010
- Liu, Y., and Priest, D. G. (1996) *Cell. Pharmacol.* **3**, 405–408
- Riordan, F. S., Foroni, L., Hoffbrand V., Mehta A. B., and Wickremasinghe R. G. (1998) *FEBS Lett.* **435**, 195–198
- Schiavone, N., Rosini, P., Quattrone, A., Donnini, M., Lapucci, A., Citti, L., Bevilacqua, A., Nicolin, A., and Capaccioli, S. (2000) *FASEB J.* **14**, 174–184
- Bandyopadhyay, S., Sengupta, T., Fernandes, D., and Spicer, E. K. (2003) *Biochem. Pharmacol.* **66**, 1151–1162
- Jacobsen, A., and Peltz, S. W. (1996) *Annu. Rev. Biochem.* **65**, 693–739
- Wilson, T., and Treisman, R. (1988) *Nature* **336**, 396–399
- Shyu, A.-B., Belasco, J. G., and Greenberg, M. E. (1991) *Genes Dev.* **5**, 221–231
- Gao, G., Wilusz, C. J., Peltz, S. W., and Wilusz, J. (2001) *EMBO J.* **20**, 1134–1143
- Fan, X. C., and Steitz, J. A. (1998) *EMBO J.* **17**, 3448–3460
- Peng, S. S., Chen, C. Y., Xu, N., and Shyu, A. B. (1998) *EMBO J.* **17**, 3461–3470
- Zhang, W., Wanger, B. J., Ehrenman, K., Schaefer, A. W., DeMaria, C. T., Crater, D., DeHaven, K., Long, L., and Brewer, G. (1993) *Mol. Cell. Biol.* **13**, 7652–7665
- Carballo, E., Lai, W. S., and Blackshear, P. J. (1998) *Science* **281**, 1001–1005
- Lai, W. S., Carballo, E., Strum, J. R., Kennington, E. A., Phillips, R. S., and Blackshear, P. J. (1999) *Mol. Cell. Biol.* **19**, 4311–4323
- Raghavan, A., Robison, R. L., McNabb, J., Miller, C. R., Williams, D. A., and Bohjanen, P. R. (2001) *J. Biol. Chem.* **276**, 47958–47965
- Chen, C.-Y., Gherzi, R., Ong, S.-E., Chan, E. L., Rajimakers, R., Pruijn, G. J. M., Stoeklin, G., Moroni, C., Mann, M., and Karin, M. (2001) *Cell* **107**, 451–464
- Mukherjee, D., Gao, M., O'Connor, J. P., Rajimakers, R., Pruijn, G., Lutz, C. S., and Wilusz, J. (2002) *EMBO J.* **21**, 165–174
- Donnini, N., Lapucci, A., Papucci, L., Witort, E., Tempestini, A., Brewer, G., Bevilacqua, M., Nicolin, A., Capaccioli, S., and Schiavone, N. (2001) *Biochem. Biophys. Res. Commun.* **287**, 1063–1069
- Lapucci, A., Donnini, M., Papucci, L., Witort, E., Tempestini, A., Bevilacqua, M., Nicolin, A., Brewer, G., Schiavone, N., and Capaccioli, S. (2002) *J. Biol. Chem.* **277**, 16139–16146
- Gluick, T. C., and Draper, D. E. (1994) *J. Mol. Biol.* **241**, 246–262
- Tholanikunnel, B. G., Raymond, J. R., and Melbon, C. C. (1999) *Biochemistry* **38**, 15564–15572
- Yang, C., Maignel, D. A., and Carrier, F. (2002) *Nucleic Acids Res.* **30**, 2251–2260
- Shyu, A.-B., Greenberg, M. E., and Belasco, J. G. (1989) *Genes Dev.* **3**, 60–72
- Ford, L. P., and Wilusz, J. (1999) *Methods Companion Methods Enzymol.* **17**, 21–27
- Altschul, S. F., Madden, T. L., Schaffer, A. A., Zhang, Z., Miller, W., and Lipman, D. J. (1997) *Nucleic Acids Res.* **25**, 3389–3402

29. Bugler, B., Bourbon, H., Lapeyre, B., Wallace, M. O., Chang, J.-H., Amalric, F., and Olson, M. O. J. (1987) *J. Biol. Chem.* **262**, 10922–10925
30. Dehlin, E., Wormington, M., Körner, C. G., and Wahle, E. (2000) *EMBO J.* **19**, 1079–1086
31. Körner, C. G., Wormington, M., Muckenthaler, M., Schneider, S., Dehlin, E., and Wahle, E. (1998) *EMBO J.* **17**, 5427–5437
32. Srivastava, M., and Pollard, H. B. (1999) *FASEB J.* **13**, 1911–1922
33. Ginisty, H., Sicard, H., Roger, B., and Bouvet, P. (1999) *J. Cell Sci.* **112**, 761–772
34. Ginisty, H., Amalric, F., and Bouvet, P. (1998) *EMBO J.* **17**, 1476–1486
35. Gordon, G. (1987) *Nature* **329**, 489–490
36. Borer, R. A., Lehner, C. F., Eppenberger, H. M., and Nigg, E. A. (1989) *Cell* **5**, 379–390
37. Bouche, G., Gas, N., Prats, H., Baldin, V., Tauber, J. P., Teissie, J., and Amalric, F. (1987) *Proc. Natl. Acad. Sci. U. S. A.* **84**, 6770–6774
38. Hanakahi, L. A., Dempsey, L. A., Li, M.-J., and Maizels, N. (1997) *Proc. Natl. Acad. Sci. U. S. A.* **94**, 3605–3610
39. Chen, C.-Y., Gherzi, R., Anderson, J. S., Gaietta, G., Jürchott, K., Royer, H.-D., Mann, M., and Karin, M. (2000) *Genes Dev.* **14**, 1236–1248
40. Malter, T. S. (2001) *J. Neurosci. Res.* **66**, 311–316
41. Skalweit, A., Doller, A., Huth, A., Kähne, T., Persson, P. B., and Thiele, B.-J. (2003) *Circ. Res.* **92**, 419–427
42. Ceman, S., Brown, V., and Warren, S. T. (1999) *Mol. Cell. Biol.* **19**, 7925–7932
43. Zaidi, S. H., and Malter, J. S. (1994) *J. Biol. Chem.* **269**, 24007–24013
44. Westmark, C. J., and Malter, J. S. (2001) *J. Biol. Chem.* **276**, 1119–1126
45. Allain, F. H., Bouvet, P., Dieckmann, T., and Feigon, J. (2000) *EMBO J.* **19**, 6870–6881
46. Bialojan, C., and Takai, A. (1988) *Biochem. J.* **256**, 283–290
47. Huang, Y., Sheikh, M. S., Fornace, A. J., Jr., and Holbrook, N. J. (1999) *Oncogene* **18**, 3431–3439
48. Derenzini, M., Sirri, V., Trere, D., and Ochs, R. L. (1995) *Lab. Invest.* **73**, 497–502
49. Zhou, G., Seibenhener, M. L., and Wooten, M. W. (1997) *J. Biol. Chem.* **272**, 31130–31137
50. Schneider, H. R., Mieskes, G., and Issinger, O. G. (1989) *Eur. J. Biochem.* **180**, 449–455
51. Morimoto, H., Okamura, H., and Haneji, T. (2002) *J. Histochem. Cytochem.* **50**, 1187–1193
52. Schiff, P. B., and Horwitz, S. B. (1980) *Proc. Natl. Acad. Sci. U. S. A.* **77**, 1561–1565
53. Guy, G. R., Cao, X., Chua, S. P., and Tan, Y. H. (1992) *J. Biol. Chem.* **267**, 1846–1852
54. Harris, N. L., Stein, H., Coupland, S. E., Hummel, M., Favera, R. D., Pasqualucci, L., and Chan, W. C. (2001) *Hematology* **194**–220
55. Mi, Y. C., Thomas, S. D., Xu, X. H., Casson, L. K., Miller, D. M., and Bates, P. J. (2003) *J. Biol. Chem.* **278**, 8572–8579